Journal of Magnetic Resonance **148,** 121–125 (2001)
doi:10.1006/jmre.2000.2217, available online at http://www.idealibrary.com on IDEAL®

Rotating Frame Analog of Spin-Locking and Spin–Lattice Relaxation in the Doubly Rotating Frame

Noriyuki Tabuchi and Hiroshi Hatanaka*

*Graduate School of Natural Science and Technology and *Department of Physics, Faculty of Education, Kanazawa University, Kanazawa 920-1192, Japan*

Received June 19, 2000; revised September 14, 2000

The present paper reports the achievement of the rotating-frame analog of spin-locking and its application to the precise measurements of the spin–lattice relaxation time T_{1DR} in the doubly rotating frame. After the magnetization is aligned along the resonant RF field H_1, a pulse sequence of a low-frequency oscillating magnetic field at exact resonance is applied perpendicular to H_1. We have overcome several technical difficulties arising from the fact that the rotating-wave approximation is not valid for the low-frequency field. We have theoretically derived an expression of T_{1DR}^{-1} due to fluctuating magnetic dipole interactions in the weak collision case and found an important relation among the spin–lattice relaxation rates T_1^{-1}, $T_{1\rho}^{-1}$, and T_{1DR}^{-1}. This relation can be used to ascertain whether the relaxation is only due to the fluctuating magnetic dipole interactions between like spins. The experiment was carried out on ^{1}H nuclei in tetramethylammonium iodide $(CH_3)_4NI$ and the temperature dependence of T_{1DR}^{-1} was measured together with that of T_1^{-1} and $T_{1\rho}^{-1}$. The activation energies and the preexponential factors of Arrhenius expressions of the correlation times are newly determined.

Key Words: **spin-locking; spin–lattice relaxation; double resonance; $(CH_3)_4NI$; rotating wave approximation.**

1. INTRODUCTION

Nuclear spin-locking, which plays important roles in fundamental studies such as double resonance (*1*) and adiabatic demagnetization in the rotating frame (*2*), has been used for various NMR investigations. The widest application of it is the measurement of the spin–lattice relaxation time $T_{1\rho}$ in the rotating frame, which is valuable because $T_{1\rho}$ is sensitive to molecular motions whose correlation times are longer than the Larmor period in the static magnetic field.

The present paper is concerned with an extension of the technique to the rotating frame. We report for the first time, to our knowledge, an achievement of a rotating-frame analog of the spin-locking (RASL) and its application to the precise measurement of the spin–lattice relaxation time T_{1DR} in the doubly rotating frame (DRF). The experiment is performed on ^{1}H nuclei in tetramethylammonium (TMA) iodide $(CH_3)_4NI$. Two strong oscillating magnetic fields are used. One is a RF field and the other a low-frequency (LF) field, both of which are sufficiently strong compared with the local field (*3*) and at exact resonance. We have confirmed the achievement of the RASL experimentally as described in Section 2. The DRF treated in this study is rigorously a triply rotating frame, but under our experimental conditions it is close to the ordinary DRF which is rotating simultaneously around the static magnetic field H_0 and the RF field H_1 at respective resonance frequencies. The details will be described in Section 3.

Although the possibility of the measurement of T_{1DR} using the RASL can be expected as an extension of the method of measuring $T_{1\rho}$, the precise measurement is not guaranteed because of several technical problems. The most serious one is the fact that the intensity H_2 of the LF field is not so small compared with that of H_1 of the RF field and, therefore, the rotating-wave approximation fails for the LF field, namely the counter- (the nonresonant) rotating LF field becomes effective. It produces not only the static effect of the well-known Bloch–Siegert shift (*4*) but also a dynamic one, which may interfere with the measurement of T_{1DR}. However, we show that T_{1DR} can be measured with a good accuracy by the RASL even when such a strong LF field is used.

We have theoretically derived an expression of T_{1DR}^{-1} due to fluctuating magnetic dipole interactions in the weak collision case and an important relation among the spin–lattice relaxation rates T_1^{-1} (laboratory frame), $T_{1\rho}^{-1}$, and T_{1DR}^{-1}. This relation is verified by measuring temperature dependences of these relaxation rates, and the activation energies E_a and the preexponential factors τ_0 of Arrhenius expressions of the correlation times are newly determined as described in Section 3.

In connection with the experiment of the RASL, we have also observed the rotating frame analogs (RAs) of free decay, transient nutation, and rotary saturation using the strong LF field. To our knowledge, no report has been published on experimental studies not only of the RASL but also of other RA phenomena performed by using such a strong LF field. Several studies reported so far (*5–10*) have been performed using LF (or audiofrequency) fields which are much weaker than the local field.

2. EXPERIMENTAL METHOD AND RESULTS ON THE RASL

The RASL experiment was performed using the pulse sequences illustrated in Fig. 1 with the RF field H_1 at the

1090-7807/01 $35.00

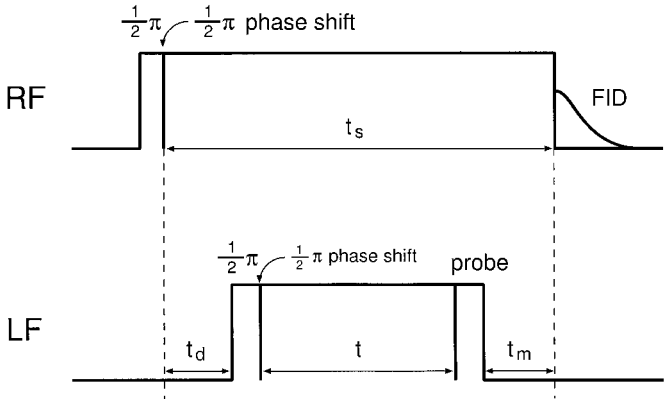

FIG. 1. Pulse sequences for the RASL. The upper and the lower sequences are for the RF and the LF fields, respectively. The delay time t_d and the time margin t_m are 200–300 μs. The phases of the second RF and the second LF pulses are shifted by $\frac{1}{2}\pi$ with respect to the first ones.

frequency $\omega_0/2\pi = 27$ MHz and with the LF field H_2 at the frequency $\omega_1/2\pi$ of about 90 kHz on ^{1}H nuclei in a polycrystalline sample of $(CH_3)_4NI$. The intensity H_2 is 5–6 Oe for $H_1 \simeq 20$ Oe. After the magnetization is aligned along H_1 by the well-known spin-locking procedure (upper trace) (*1, 2*), we apply the $\frac{1}{2}\pi$ LF pulse followed by the spin-locking LF pulse (the second LF pulse) whose phase is shifted by $\frac{1}{2}\pi$ with respect to the first one (lower trace). The third LF pulse is the probe pulse by which the RASL magnetization, namely the magnetization along H_2, is converted to the magnetization M_1 along H_1 which can be measured from the free induction decay (FID) signal just after the second RF pulse. The phase of the probe pulse is shifted by π with respect to the first one. The relaxation of the RASL magnetization is observed by changing both the lengths of the LF and the RF pulses (t and t_s) at the same time, keeping the delay time t_d and the time margin t_m (shown in Fig. 1) constant.

A typical experimental result is shown in Fig. 2. Open circles in Fig. 2 indicate that the RASL magnetization is maintained for a very long time compared with the transverse decay time of the order of 100 μs, namely the RASL is really achieved. From the decay of the RASL magnetization the spin–lattice relaxation time T_{1DR} can be measured. Closed circles show the decay of the magnetization along H_1 in the singly rotating frame observed at the same intensity H_1.

We also carried out an experiment of the RA of rotary saturation by introducing a weak sinusoidal amplitude modulation to the RF field during the spin-locking LF pulse. The amplitude modulation produces an oscillating magnetic field perpendicular to H_2 in the DRF analogous to the usual rotary saturation (*5, 6*). We observed that the RASL magnetization decreases when the modulation frequency is equal to or near γH_2, where γ is the gyromagnetic ratio of the nuclei. This experimental result also shows the achievement of the RASL.

In the measurement of T_{1DR} using the RASL, there exist at least two experimental problems to be solved. Although the Bloch–Siegert shift is negligible in our experimental condition, the dynamic effect of the counterrotating LF field may affect the measurement. Actually, it appears on a signal of the RA of transient nutation observed by applying a single LF pulse during the usual spin-locking. We found that the nutation signal contains small oscillations at the angular frequencies of $2\omega_1 \pm \gamma H_2$ superimposed on the main oscillation at the angular frequency γH_2. In the measurement of T_{1DR}, however, the oscillations due to the dynamic effect do not appear in the relaxation curve when the magnitude $(H_2/2H_1)^n$ with $n \geqq 2$ is negligibly small. We confirmed this both theoretically and experimentally. The details will be reported later.

The other problem is the phase dependence of the intensity H_2 of the probe pulse arising from the fact that its duration is comparable to the period $2\pi/\omega_1$. Since the LF pulses are coherent, the initial LF phase of the probe pulse changes periodically as the probe pulse delays and, therefore, a small fluctuation appears in the observed decay curve. The Fourier spectrum of the fluctuation, which was observed by fixing the initial phase of the LF pulse sequence, consisted of two main lines at the angular frequencies ω_1 and $2\omega_1$ (not at $2\omega_1 \pm \gamma H_2$). This result implies that the fluctuation can be eliminated by averaging four magnitudes of M_1 obtained by shifting the initial phase of the LF pulse sequence by amounts of $\frac{1}{2}\pi$, and actually it was almost eliminated. The curve shown by the open circles in Fig. 2 is obtained by this averaging method.

In order to adjust the frequency ω_1 to the exact resonance, we used the RA of FID signals. These were observed by reducing the amplitude of the spin-locking LF pulse in Fig. 1 to zero and plotting the magnitude of M_1 as a function of the separation between two LF pulses. The averaging method mentioned above was also used. When $\omega_1 = \gamma H_1$, the decay of the RA of the FID signal observed coincides with that of the

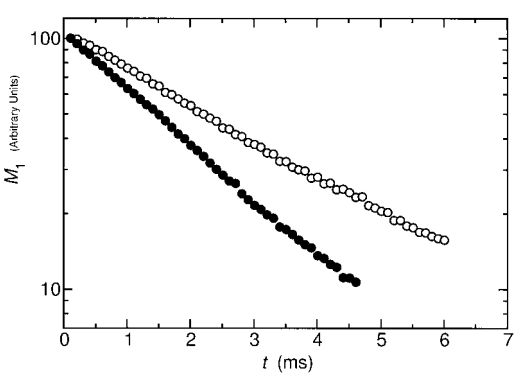

FIG. 2. Decay of the RASL magnetization due to the spin–lattice relaxation in the DRF (open circles). This is observed with $\omega_1/2\pi = 88.9$ kHz and $H_2 = 5.2$ Oe at room temperature. The relaxation time T_{1DR} estimated from the curve is about 2.96 ms. Closed circles show the relaxation in the singly rotating frame observed with the same RF field at the same temperature. The estimated $T_{1\rho}$ ($T_{1\rho}^{\ddagger}$) is 1.94 ms.

usual transient nutation (*11*). When ω_1 is slightly shifted from γH_1, the decay becomes apparently faster, and an oscillatory behavior is observed for a larger frequency offset.

The NMR spectrometer used is homemade. A 300-W RF amplifier (THAMWAY A55-3602MR) produces the strong RF field H_1 in the RF sample coil of 15-mm diameter and 18-mm length. The LF pulse was generated by a combination of an oscillator (HP 33120A) and gated preamplifier with phase shifters (homemade). The LF pulse was amplified by a 50-W audioamplifier and supplied to Helmholtz coils of 32-mm diameter and 18-mm separation. The equipment is devised so that no DC voltage is applied to the coils. The volume of the sample, which was a commercial product was about 0.3 cm^3. The sample was not sealed but was placed in an open sample tube that was well wrapped with Teflon tape. A copper–Constantan thermocouple was inserted inside the sample. We could maintain the temperature of the sample within ± 1 K over the range of 210 to 400 K even under a long RF pulse with the duration of about 200 ms and with the intensity H_1 of about 20 Oe.

3. ON THE RELAXATION RATE T_{1DR}^{-1} IN THE DRF

(1) Derivations of the Expression of T_{1DR}^{-1} and Its Relation to T_1^{-1} and $T_{1\rho}^{-1}$

We start from the equation of motion for the density matrix ρ' of the spin system $I(=\Sigma I_j)$ aligned along H_1 ($\|z$-axis) in a frame rotating around H_0 at the angular frequency ω_0 ($=\gamma H_0$), where the Hamiltonian includes the fluctuating magnetic dipole interactions between like spins. According to the procedures described in Ref. (*12*), the equation of motion for ρ' is first transformed to that in the reference frame rotating at the angular frequency ω_1 in the reverse sense to the nuclear precession around the z-axis, and then the rotating frame is tilted around its y-axis through an angle θ so that its z-axis becomes parallel to the effective field of the intensity $[(\omega_1/\gamma + H_1)^2 + H_2^2]^{1/2}$. Finally the equation of motion is transformed to that in the reference frame rotating at the angular frequency $2\omega_1$ in the same sense as the nuclear precession around the tilted z-axis. The final reference frame is that rotating triply at ω_0, ω_1, and $2\omega_1$.

In our experimental condition, θ is so small that

$$\exp(\pm i\theta) \cong 1 \pm i\theta, \qquad [1]$$

where $\theta \cong H_2/2H_1$, and all the terms including θ^n with $n \geqq 2$ can be neglected in the following calculation. In this case the final reference frame is close to the ordinary DRF rotating at ω_0 around H_0 and at ω_1 around H_1 in the same sense as the nuclear precession. There is no axis in common with the singly rotating frame.

Next, we transform the equation of motion for the density matrix ρ'' in the triply rotating frame to that for the density matrix $\rho^{\ddagger}$ presented by

$$\rho^{\ddagger}(t) = \exp(-i\gamma H_2 I_z t)\exp\left(-i\frac{\pi}{2}I_y\right)\rho''(t) \times \exp\left(i\frac{\pi}{2}I_y\right)\exp(i\gamma H_2 I_z t). \qquad [2]$$

From this equation of motion, the master equation for $\rho^{\ddagger}$ can be derived by a well-known perturbation treatment with several assumptions (*12*). By a standard calculation starting from the master equation under the condition $\omega_0 \gg \omega_1$, we obtain

$$T_{1DR}^{-1} = \frac{3}{32}I(I+1)\hbar^2\gamma^4\Big\{J^{(0)}(2\omega_2) + \frac{1}{4}\sum_{n=-2(\neq 0)}^{2}(1-2n\theta)J^{(0)}(2\omega_1 + n\omega_2) + 28J^{(1)}(\omega_0) + 10J^{(2)}(2\omega_0)\Big\}, \qquad [3]$$

where $\omega_2 = \gamma H_2$. $J^{(m)}(\omega)$'s ($m = 0, 1, 2$) in Eq. [3] are the spectral density functions, the explicit forms of which are given in Ref. (*13*), for example. When $\theta = 0$, Eq. [3] coincides with the expression of T_{1DR}^{-1} in the ordinary DRF. By using the following approximation,

$$J^{(0)}(2\omega_1 + n\omega_2) \cong J^{(0)}(2\omega_1)\{1 - n\Delta(\omega_2)\}, \quad (n = \pm 1, \pm 2), \qquad [4]$$

where $\Delta(\omega_2)$ is fairly small compared with unity, the sum of four terms with $J^{(0)}(2\omega_1 + n\omega_2)$ in Eq. [3] becomes $J^{(0)}(2\omega_1)$ because the amount of $5\theta\Delta(\omega_2)$ is negligibly small. Thus, Eq. [3] is rewritten as

$$T_{1DR}^{-1} \cong \frac{3}{2}I(I+1)\hbar^2\gamma^4\Big\{\frac{1}{16}J^{(0)}(2\omega_2) + \frac{1}{16}J^{(0)}(2\omega_1) + \frac{7}{4}J^{(1)}(\omega_0) + \frac{5}{8}J^{(2)}(2\omega_0)\Big\}. \qquad [5]$$

Equation [5] is also derived from Eq. [3] with $\theta = 0$ and, therefore, shows that the relaxation rate T_{1DR}^{-1} measured under the condition in Eq. [1] can be regarded as that in the ordinary DRF. So, we use simply the term DRF in the following discussion, ignoring the difference between the triply rotating frame and the ordinary DRF.

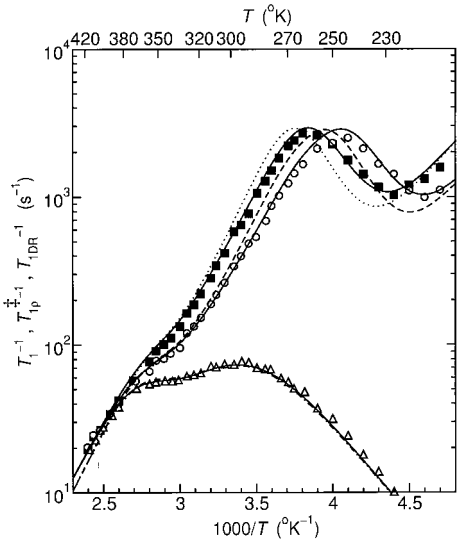

FIG. 3. Temperature dependences of the relaxation rates. Circles, triangles, and squares show the experimental relaxation rates T_{1DR}^{-1}, T_1^{-1}, and $T_{1\rho}^{\ddagger -1}$, where $\omega_1/2\pi = 89.3$ kHz and $H_2 = 6.4$ Oe. Solid lines are the theoretical curves for the respective relaxation rates plotted with our values of E_a and τ_0. The broken, dotted, and broken–dotted lines are the theoretical curves for T_{1DR}^{-1}, $T_{1\rho}^{\ddagger -1}$, and T_1^{-1} which are plotted with the values given by Albert *et al.* (*16*). The broken line above about 380 K shows the superposition of the broken, dotted, and broken–dotted lines.

As it is well known, the relaxation rates T_1^{-1} and $T_{1\rho}^{-1}$ due to the same relaxation mechanism are given by (*12–14*).

$$T_1^{-1} = \frac{3}{2} I(I+1)\hbar^2\gamma^4\{J^{(1)}(\omega_0) + J^{(2)}(2\omega_0)\},$$

$$T_{1\rho}^{-1} = \frac{3}{2} I(I+1)\hbar^2\gamma^4\left\{\frac{1}{4} J^{(0)}(2\omega_1) + \frac{5}{2} J^{(1)}(\omega_0) + \frac{1}{4} J^{(2)}(2\omega_0)\right\}. \quad [6]$$

In the high temperature limit, where the correlation times are much shorter than the Larmor period $2\pi/\omega_0$, spectral density functions $J^{(m)}(\omega)$'s in Eqs. [5] and [6] are equal to $J^{(m)}(0)$ and, then, T_{1DR}^{-1} becomes equal to both T_1^{-1} and $T_{1\rho}^{-1}$, where $J^{(0)}(0)$: $J^{(1)}(0)$:$J^{(2)}(0) = 6$:1:4 (*12, 15*).

The following equations are derived from Eqs. [5] and [6];

$$4T_{1DR}^{-1} - T_{1\rho}^{\ddagger -1} - 2T_1^{-1} = T_{1\rho}^{\dagger -1}, \quad [7]$$

and

$$2T_{1DR}^{-1} - T_{1\rho}^{\ddagger -1} - T_1^{-1} = \frac{3}{16} I(I+1)\hbar^2\gamma^4 \times \{J^{(0)}(2\omega_2) - J^{(0)}(2\omega_1)\}, \quad [8]$$

where $T_{1\rho}^{\dagger -1}$ means the relaxation rate in the singly rotating frame given by replacing ω_1 by ω_2 in the expression of $T_{1\rho}^{-1}$ in Eqs. [6], and $T_{1\rho}^{\ddagger -1}$ is the relaxation rate in the singly rotating frame measured at the same H_1 as in the T_{1DR}^{-1} measurement. (Rigorously, the RF intensity for $T_{1\rho}^{\ddagger -1}$ is higher than this intensity by an amount due to the Bloch–Siegert shift, which can be neglected.) The theoretical result, Eq. [7], is an important relation among the spin–lattice relaxation rates and can be used to ascertain whether the relaxation phenomenon under consideration is only due to the fluctuating magnetic dipole interactions between like spins. Equation [8] indicates that T_{1DR}^{-1} is equal to the mean value of T_1^{-1} and $T_{1\rho}^{\ddagger -1}$ when $J^{(0)}(2\omega_2) = J^{(0)}(2\omega_1)$.

(2) Experimental Results and Discussions

Open circles in Fig. 3 indicate the experimental temperature dependence of T_{1DR}^{-1}. In the high temperature region (over about 380 K), the curve for T_{1DR}^{-1} coincides with those for T_1^{-1} and $T_{1\rho}^{\ddagger -1}$, shown by the triangles and the squares as predicted by the theory. The temperature where T_{1DR}^{-1} is maximum is lower than the corresponding temperature for $T_{1\rho}^{\ddagger -1}$, and these temperatures are below the room temperature. From the expressions of T_{1DR}^{-1} and $T_{1\rho}^{-1}$ with the assumption of BPP spectral density function (*15*), it is expected that one of the correlation times of the proton motions at the maximum of T_{1DR}^{-1} is nearly equal to $(2\omega_2)^{-1}$ and the corresponding one at the maximum of $T_{1\rho}^{\ddagger -1}$ to $(2\omega_1)^{-1}$.

The temperature dependence of the value of $4T_{1DR}^{-1} - T_{1\rho}^{\ddagger -1} -$

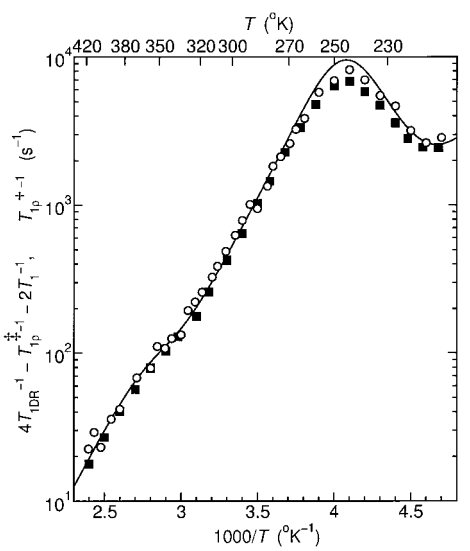

FIG. 4. Temperature dependence of $4T_{1DR}^{-1} - T_{1\rho}^{\ddagger -1} - 2T_1^{-1}$ and that of $T_{1\rho}^{\dagger -1}$. Circles show the curve for $4T_{1DR}^{-1} - T_{1\rho}^{\ddagger -1} - 2T_1^{-1}$ obtained from the respective experimental relaxation rates at the same temperatures which are shown in Fig. 3, and squares show that of $T_{1\rho}^{\dagger -1}$ measured by the RF field of the intensity equal to H_2. The good agreement between the curves shows the validity of Eq. [7]. The solid line is the theoretical curve plotted with our values of E_a and τ_0.

$2T_1^{-1}$ calculated from the respective experimental data in Fig. 3 was in excellent agreement with that of $T_{1\rho}^{\dagger -1}$ measured at the RF intensity equal to H_2, as shown in Fig. 4. The experimental result verifies the validity of Eq. [7]. The curve for T_{1DR}^{-1} shown by the open circles in Fig. 3 is clearly different from that for $T_{1\rho}^{\dagger -1}$ shown by the squares in Fig. 4 below about 380 K, although the temperatures at these maxima are almost equal.

In the range from 270 to 420 K, the curves for $T_{1\rho}^{\ddagger -1}$ and $T_{1\rho}^{\dagger -1}$ shown by the squares in Figs. 3 and 4 well coincide with each other, which means that $J^{(0)}(2\omega_2) = J^{(0)}(2\omega_1)$. As expected from Eq. [8], the values of T_{1DR}^{-1} shown by the open circles in Fig. 3 are in good agreement with the mean values of T_1^{-1} and $T_{1\rho}^{\ddagger -1}$ shown by the triangles and the squares in this temperature range.

Albert *et al.* reported that the relaxation mechanism in $(CH_3)_4NI$ can be interpreted by the fluctuating magnetic dipole interactions between the proton spins with two correlation times (*16*). In order to confirm that Eq. [5] describes the experimental curve for T_{1DR}^{-1} in Fig. 3, we derived an explicit expression of T_{1DR}^{-1} from Eq. [5] by a similar procedure to that of Albert *et al.* and plotted the temperature dependence using their values of E_a, τ_0, A, and B (*16*). However, the agreement of the obtained theoretical curve (broken line in Fig. 3) with the experimental one is not so good. The dotted line in Fig. 3 is a theoretical curve for $T_{1\rho}^{\ddagger -1}$ obtained in a similar manner by using their values and explicit expression of $T_{1\rho}^{-1}$. The disagreement is also observed. In order to obtain the better agreement we adjusted the values of E_a and τ_0, keeping the values of A and B unchanged. The best agreements for T_{1DR}^{-1} and $T_{1\rho}^{\ddagger -1}$ are obtained when the values $E_a = 5.56$ kcal and $\tau_0 = 2.6 \times 10^{-13}$ s for CH_3 group rotation and $E_a = 10.0$ kcal and $\tau_0 = 3.5 \times 10^{-15}$ s for Cation tumbling are used, and the results are shown by the solid lines. The agreement is quite satisfactory.

A remarkable difference between our values and theirs is in τ_0 for the Cation tumbling. Our value is about 4.4 times as large as their value and nearly equal to the corresponding one in TMA bromide (*16*). The longer correlation times are probably sensitively detected by our experimental method.

The newly determined values lead to the theoretical curve (solid line in Fig. 3) for T_1^{-1}, which is in excellent agreement with experimental results. The agreement is better at temperatures above about 380 K than the broken–dotted line which is derived from their values, although the difference is small.

To further check the validity of our values, we tried to interpret the experimental temperature dependence of T_1 by Albert *et al.* taken at $\omega_0/2\pi = 25.3$ MHz (*16*) using our values. The agreement between our theoretical results and their experimental ones was very good (not shown in the figure).

We also obtained, with our values of E_a and τ_0, the theoretical curve of $4T_{1DR}^{-1} - T_{1\rho}^{\ddagger -1} - 2T_1^{-1}$ or $T_{1\rho}^{\dagger -1}$ as shown by the solid line in Fig. 4, which is in excellent agreement with the experimental curves.

Although we have applied the LF magnetic field in this study, the RASL and the T_{1DR} measurement are also possible by introducing a strong frequency or phase modulation to H_1 instead. This method may be more convenient if a sinusoidal modulation is applied, because a single sample coil can essentially produce a better homogeneous LF field.

ACKNOWLEDGMENT

The authors are indebted to Mr. M. Nishimoto for his assistance in instrumentation.

REFERENCES

1. S. R. Hartmann and E. L. Hahn, Nuclear double resonance in the rotating frame, *Phys. Rev.* **128,** 2042–2053 (1962).
2. A. G. Anderson and S. R. Hartmann, Nuclear magnetic resonance in the demagnetized state, *Phys. Rev.* **128,** 2023–2041 (1962).
3. M. Goldman, "Spin Temperature and Nuclear Magnetic Resonance in Solids," Clarendon Press, Oxford, 1970.
4. F. Bloch and A. Siegert, Magnetic resonance for nonrotating fields, *Phys. Rev.* **57,** 522–527 (1940).
5. A. G. Redfield, Nuclear magnetic resonance saturation and rotary saturation in solids, *Phys. Rev.* **98,** 1787–1809 (1955).
6. J. R. Franz and C. P. Slichter, Studies of perturbation theory and spin temperature by rotary saturation of spins, *Phys. Rev.* **148,** 287–298 (1966).
7. M. Kunitomo and T. Hashi, Adiabatic demagnetization in the doubly rotating frame, *Phys. Lett.* **34A,** 157–158 (1971).
8. M. Kunitomo and T. Hashi, Zeeman and dipole temperatures in the rotating frame: Effects of prolonged irradiation, *Phys. Lett.* **38A,** 461–462 (1972).
9. H. Hatanaka and T. Hashi, Spin-locking, spin-locked echo and rotary saturation associated with a two-quantum transition in a multilevel NMR system, *Phys. Lett.* **67A,** 183–185 (1978).
10. A. E. Mefed, Nuclear magnetic resonance in a modulated effective field, *Zh. Eksp. Teor. Fiz.* **86,** 302–311 (1984) [*Sov. Phys. JETP* **59,** 172–178 (1984)].
11. H. C. Torrey, Transient nutations in nuclear magnetic resonance, *Phys. Rev.* **76,** 1059–1068 (1949).
12. A. Abragam, "The Principles of Nuclear Magnetism," Oxford Univ. Press, Oxford, 1961.
13. G. P. Jones, Spin–lattice relaxation in the rotating frame: Weak-collision case, *Phys. Rev.* **148,** 332–335 (1966).
14. D. Wolf, "Spin-Temperature and Nuclear-Spin Relaxation in Matter," Clarendon Press, Oxford, 1979.
15. N. Bloembergen, E. M. Purcell, and R. V. Pound, Relaxation effects in nuclear magnetic resonance absorption, *Phys. Rev.* **73,** 679–712 (1948).
16. S. Albert, H. S. Gutowsky, and J. A. Ripmeester, On a T_1 and $T_{1\rho}$ study of molecular motion and phase transitions in the tetramethylammonium halides, *J. Chem. Phys.* **56,** 3672–3676 (1972).